Thermodynamics, Orientational Order and Elasticity of Strained Liquid Crystalline Melts and Elastomers†

Folusho T. Oyerokun and Kenneth S. Schweizer*

Department of Materials Science and Engineering and Frederick Seitz Materials Research Laboratory, University of Illinois, 1304 West Green Street, Urbana, Illinois 61801

Received: September 24, 2004

A microscopic polymer liquid-state theory has been developed for the structure, thermodynamics and mechanical properties of strained liquid crystalline elastomers. The theory captures the experimentally observed phenomenon of spontaneous distortion and establishes a direct correlation between it and the nematic order parameter. Strain induced softening of the elastic modulus is predicted to emerge due to coupling of the induced orientational order and anisotropic interchain excluded volume interactions. Comparison of our results with limited experiments shows good qualitative and sometimes quantitative agreement. The theory predicts that deformation in the liquid crystalline state results in an increase of the amplitude of density fluctuations (compressibility) which becomes more pronounced as chain degree of polymerization and/or segmental density are decreased.

I. Introduction

Liquid crystalline elastomers (LCE) have been the subject of intense study over the past decade or so because of their unusual optical and mechanical properties[1−3] which arise from the coupling of liquid crystallinity (orientation) and rubber elasticity (strain/deformation). LCE are formed when a main chain or side chain liquid crystal polymer is crosslinked, either in the nematic or isotropic phase, to form a network. To ensure that a sample with a uniform director is formed (monodomain), the crosslinking is often done after alignment by an external electric, magnetic or mechanical field.[1,3]

When an elastomer is cooled below the isotropic−nematic phase transition temperature of the non-crosslinked liquid crystalline polymer, the network strands undergo alignment. Because the chains are connected via the chemical crosslinks, this microscopic change is transmitted globally, resulting in an increase in the sample length along the director and a corresponding reduction in the perpendicular direction. The reverse trend occurs when the sample is heated. This phenomenon, termed spontaneous distortion, has been touted in applications such as temperature sensors, temperature-controlled actuators[1,4] and artificial muscles.[5] Another consequence of chain alignment is a reduction in the free energy cost of mechanical deformation, i.e., a decrease in the elastic modulus or strain softening. Also, because the director in a monodomain sample is anchored to the rubber matrix, thermal fluctuation are greatly suppressed, resulting in optical clarity.[1] This property, as well as mechanical stability, is being exploited by Finkelmann and co-workers in the design of optical lenses.[1]

The first molecular theory of nematic elastomers was proposed by Warner and co-workers[1,3] and is an extension of the classical rubber elasticity model with allowance for chain anisotropy. The chain equilibrium conformation is assumed to be described by an anisotropic Gaussian distribution with an effective step tensor representing the nematic ordering in the network. The theory explicitly ignores the consequences of intermolecular interactions or entanglements which are known to be important and can lead to qualitatively new behavior in flexible chain networks.[6,7] Treatment of intermolecular effects beyond the classical framework is a significant challenge, particularly in the presence of the quenched disorder associated with chemical crosslinks. Prior attempts have relied on semi-microscopic and phenomenological models,[8−12] while a rigorous statistical mechanical treatment remains elusive. For example, Kutter and Terentjev have applied the Edwards tube model to treat the elasticity of entangled nematic elastomers.[13]

Recently, we developed a microscopic theory to explicitly treat interchain excluded volume interactions in strained melts and rubber networks.[14,15] The theory, an anisotropic generalization of the polymer reference interaction site model (PRISM), was used to predict structure, orientational order, thermodynamics and mechanical response in non liquid crystalline elastomers. PRISM theory predicts two nonclassical contributions to the stress or elastic modulus of a rubber network arising from intermolecular effects.[15] The first is due primarily to interchain repulsive interactions and is always positive definite. The second, associated with strain induced alignment of the chains, leads to a reduction in the free energy cost of deformation. It is the complex interplay between the two nonclassical contributions that accounts for the observed deviation from the modulus predicted by the classical models. Furthermore, because of the supralinear dependence of the nonclassical terms on segmental density, the effect of the nonclassical terms is even more pronounced in the liquid crystalline state since the required local chain rigidity implies large segmental densities. Our present goal is to extend our prior theory to monodomain liquid crystalline elastomers.

The organization of the paper is as follows. In section II, we review PRISM theory for liquid crystalline polymers and rubber networks. Application to orientational order, density fluctuations and thermodynamics in nematic elastomers is discussed in section III. Section IV addresses the unusual mechanical properties, spontaneous distortion and modulus softening, followed by comparison of our theoretical predictions with

† Part of the special issue "David Chandler Festschrift".

10.1021/jp045646i CCC: $30.25
Published on Web 01/26/2005

experiments on thermotropic liquid crystalline elastomers. The paper concludes in section V with a summary of results, limitations of the theory, and future directions. The appendices discuss similarities between our theory of nematic elastomers and the mean field theory of magnets and compares our approach with the neoclassical theory of liquid crystalline elastomers.[1,3,16]

II. PRISM Theory of Rubber Networks

A. Isotropic Polymer Liquids. PRISM theory is a generalization to polymeric liquids of the integral equation theory of small molecule fluids of Chandler and Andersen,[17,18] the reference interaction site model (RISM). PRISM theory has been successfully applied to a wide range of polymer problems, including isotropic polymer solutions, melts, blends and block copolymers,[19,20] liquid crystalline polymers,[21−23] polymer−colloid suspensions,[24] and polymer nanocomposites.[25]

In PRISM theory, a polymer chain of degree of polymerization, N, is treated as a collection of spherically symmetric interaction sites. In a coarse grained description, a site represents a few monomers within a statistical (Kühn) segment. In general, the chain conformation is strongly dependent on the balance between the intramolecular and intermolecular interactions between sites. In a dense melt the intrachain site−site probability distribution is "ideal" or Gaussian. An analytically tractable, field-theoretic-like version of PRISM models chains as uncrossable threads of zero thickness,[19,26−28] the so-called Gaussian thread limit. The corresponding single chain structure factor, or Fourier transform of the intrachain site−site probability distribution, is given by the Debye function, which is often approximated by a Lorentzian for analytical convenience:[28]

$$\omega(\vec{k}) \approx \left(\frac{1}{N} + \frac{\sigma^2 k^2}{12}\right)^{-1} \tag{1}$$

where σ is the statistical segment length. This approximation exactly captures the long and intermediate wavelength behavior.[28] In the Gaussian thread description, all the chemical specific information is buried in the dimensionless segmental density, $\rho\sigma^3$, which is related to the corresponding invariant "packing length",[29] $l_p \equiv (\rho\sigma^2)^{-1}$, as

$$\rho\sigma^3 = \frac{\sigma}{l_p} = \frac{l\sqrt{C_\infty}}{l_p} \tag{2}$$

Here, ρ is the site (or segmental) number density, l the typical chemical bond length and C_∞ the backbone characteristic ratio. The dimensionless segmental density for most flexible (non liquid crystalline) polymer melts[29] is $\approx 1-2$.

The interchain site−site pair correlation function, $g(r) \equiv 1 + h(r)$, of a homopolymer fluid is determined via solution of the generalized Ornstein−Zernike or Chandler-Andersen integral equation:[18−20]

$$h(r) = \int \mathrm{d}\vec{r}' \int \mathrm{d}\vec{r}'' \omega(|\vec{r} - \vec{r}'|) C(|\vec{r}' - \vec{r}''|)[\omega(r'') + \rho h(r'')] \tag{3}$$

Chain end effects have been ignored (all sites are treated as effectively equivalent), and $C(r)$ is the site−site intermolecular direct correlation function. For thread polymers interacting via purely repulsive hard core forces, the appropriate site−site Percus−Yevick (PY) closure is[19,20]

$$C(r) = C_0 \delta(\vec{r}) \tag{4}$$

The single unknown quantity, the direct correlation *parameter* C_0, is determined via rigorous enforcement of the pointlike excluded volume constraint, $g(r = 0) = 0$. Once the pair correlation function has been determined, connection is made with thermodynamics via the collective density fluctuation structure factor:

$$S(k) \equiv \omega(k) + \rho h(k) = \frac{1}{\omega^{-1}(k) - \rho C_0} \tag{5}$$

The zero wave-vector limit is related to the isothermal compressibility:[18,19,30] $S(0) = \rho k_B T \kappa_T = (N^{-1} - \rho C_0)^{-1}$. All thermodynamic properties can then be computed via straightforward thermodynamic integration. The pressure and free energy (in units of $k_B T$) are[14]

$$p = \int_0^{\rho_m} d\rho' \frac{1}{S(0,\rho')} \tag{6}$$

$$F = \int_0^{\rho_m} d\rho' \frac{p}{\rho'^2} \tag{7}$$

Gaussian thread PRISM,[19,20] eqs 1−5, is a coarse-grained analytic limit of PRISM theory which was originally proposed by Schweizer and Curro[26] based on an intuitive analogy with the Edwards field theory approach.[28] It was derived by Chandler for thread polymers based on a nonlocal Gaussian field theory formulation of liquid-state integral equation theory.[31] Most recently, Fuchs used exact Baxter factorization methods for random walk polymers to prove thread PRISM-PY theory rigorously emerges for nonzero thickness chain models in an appropriate segmental density regime.[32]

B. Anisotropic Polymer Liquids. PRISM theory was generalized to anisotropic polymer liquids by Pickett and Schweizer[21−23] to treat structure, thermodynamics and phase behavior of liquid crystal forming polymers. The single thread chain (or rod[23]) structure is modeled as a directed random walk with conserved mean squared radius of gyration but different step lengths in directions parallel and perpendicular to the director, i.e., the polymer can undergo pure rotation. Recently, we have generalized this approach to include chain deformation as well as orientation, and have successfully applied the theory to structure, orientational order, and mechanical response of non liquid crystalline strained rubber networks. The key results from this work[14,15] are summarized below.

A basic question that arises is the justification of a liquid-state treatment since an elastomer is not an equilibrium liquid on all length scales due to the presence of quenched chemical cross-links. However, as argued in our previous work,[14,15] equilibrium is expected to be very nearly achieved on length scales of the order of the mean distance between cross-links and smaller, the relevant scales for determining the thermodynamic consequences of intermolecular interactions. Also, on these length scales the network strand has nearly the same ideal conformational statistics as in a melt.[6,7] This motivates the treatment of a network as a strained melt of chain degree of polymerization equal to the network strand size. Further support for this simplification is the very good agreement between our theory and experiments demonstrated in earlier work.[14,15]

When a rubber material is strained, its macroscopic dimensions change, in a manner that depends on the way the sample is deformed. Consider a cubic sample of an elastomer. In uniaxial extension, the length along the strain axis increases by a factor of λ. If we assume that the deformation occurs isochorically, the other two dimensions change by a factor of

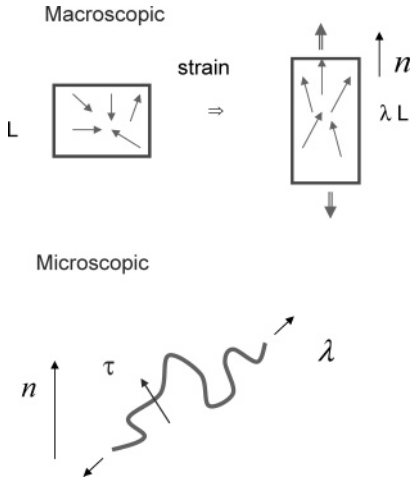

Figure 1. Schematic illustration of the macroscopic and microscopic description of deformation in a rubber network. Arrows indicate segmental bond or end-to-end vectors of network strands, λ defines the amplitude of uniaxial extensions, $\vec{n}$ indicates the nematic director, and τ is the segmental (bond) orientation order parameter.

$1/\sqrt{\lambda}$. Microscopically, each of the network strands also undergoes a deformation, often assumed to be identical to the macroscopic changes, i.e., affine.[6,7] Upon deformation, the segmental bond vectors are no longer randomly distributed as in an isotropic liquid. A measure of this deviation from isotropy is the segmental or orientational order parameter, τ, defined as

$$\tau \equiv \left\langle \frac{1}{2}[3\cos^2(\alpha) - 1] \right\rangle \tag{8}$$

where α is the angle between a bond vector and the strain (orientation) axis. The situation is illustrated in Figure 1 where a cartoon shows both the macroscopic and microscopic states, before and after deformation. By definition, in an isotropic system the segmental order parameter is zero. Clearly, the single chain structure is a function of the imposed strain and segmental orientational order. In ref 14, we derived an expression for the anisotropic single chain structure factor of a directed random walk based on the following ideas: (i) the first moment of the distribution is modeled as an anisotropic directed walk, (ii) the deformation is affine in the limit of zero alignment, and (iii) the pure alignment result is recovered in the limit $\lambda \to 1$. The resulting expression is

$$\omega(k_{||},k_{\perp};\lambda,\tau) = \left\{\frac{1}{N} + \frac{\sigma^2 k^2}{12}[1 + (3\cos^2\theta - 1)\tau]\right\} \Big/ \left\{\left\{\frac{1}{N} + \frac{\sigma^2 k^2}{12}[1 + (3\cos^2\theta - 1)\tau]\right\}^2 + \frac{\sigma^2[1 + (3\cos^2\theta - 1)\tau][k_{||}\sqrt{\lambda^2 - 1} + k_{\perp}\sqrt{\lambda^{-1} - 1}]^2}{12N}\right\} \tag{9}$$

Because of the complexity of eq 9, controlled approximations were invoked in order to analytically solve the PRISM integral equation. It was found that analytical solution is possible if the allowable strain is constrained within the wide range

$$\frac{1}{N} \ll \lambda \tag{10}$$

$$\lambda \ll \sqrt{N} \tag{11}$$

which is consistent with the chain not fully extended into a rodlike conformation nor collapsed. The free energy expression obtained, in units of k_BT, is

$$F_{\text{int}} = \frac{\ln(\rho)}{N} - \ln[(1-\tau)\sqrt{1+2\tau}] + \frac{\pi\rho\sigma^3(1-\tau)\sqrt{1+2\tau}}{6\sqrt{3N}} + \frac{\pi^2\rho^2\sigma^6(1-\tau)^2(1+2\tau)}{648} + \frac{f(1-\tau)\sqrt{1+2\tau}}{32}\left\{\frac{\pi\rho\sigma^3(1-\tau)\sqrt{1+2\tau}}{\sqrt{3N}} - \frac{4}{N}\ln\left[1 + \frac{\pi\rho\sigma^3(1-\tau)\sqrt{1+2\tau}\sqrt{N}}{12\sqrt{3}}\right]\right\} \tag{12}$$

where the function f depends in a rich manner on strain and orientational order as

$$f = \left\{6\sqrt{\tau}\left[\left(\lambda^2 - \frac{1}{\lambda}\right) - \left(\lambda^2 + \frac{2}{\lambda} - 3\right)\tau\right] + \sqrt{3}(1-\tau)\sqrt{1+2\tau}\left(\lambda^2 - \frac{1}{\lambda}\right)\ln\left[\frac{\sqrt{1+2\tau} - \sqrt{3\tau}}{\sqrt{1+2\tau} + \sqrt{3\tau}}\right]\right\} \Big/ \left\{9\tau^{3/2}(\tau-1)\sqrt{1+2\tau}\right\} \tag{13}$$

Note that $f \to 0$ in the $\lambda \to 1$ pure alignment limit.

The total free energy is the sum of the classical, non interacting entropic spring (intramolecular) contribution,[33] and the interaction or excess term, i.e.

$$F = F_{classical} + F_{\text{int}} \tag{14}$$

where the classical affine term[33] is $F_{classical} = (\lambda^2 + 2\lambda^{-1} - 3)/2N$. In the absence of strain ($\lambda = 1$), the equilibrium order parameter is found by minimizing the free energy. Below a critical segmental density, the orientational order is zero. The critical density above which a nonzero τ first occurs is a weak function of the degree of polymerization and is given by[21]

$$(\rho\sigma^3)_{NI} = \frac{9(\sqrt{3+4N} - \sqrt{3})}{\pi\sqrt{N}} \tag{15}$$

The isotropic−nematic transition segmental density increases in a finite size manner with N, and ranges between 5 and 6. Above this density, thread PRISM theory predicts a continuous (second order) phase transition marked by degeneracy between the nematic and discotic phases. The continuous nature of the transition is a consequence of the $d \to 0$ Gaussian thread model. A less coarse-grained (but far less analytically tractable) model which incorporates a nonzero chain thickness or local backbone stiffness results in a first-order phase transition and broken nematic−discotic symmetry.[21] The orientational order parameter is given by the solution of a cubic equation

$$(1-\tau)\sqrt{1+2\tau} = \frac{\rho_{NI}}{\rho} \tag{16}$$

In subsequent analysis, contact between our lyotropic based approach and thermotropic liquid crystals is made via choosing a $\rho\sigma^3$ value that corresponds to the relevant (temperature-dependent) degree of nematic order parameter in the absence of strain.

For the deformed network, the dependence of the induced segmental order on strain and material properties is found by minimizing eq 14 with respect to τ. The resulting expression is

very complex. A simple analytic form for τ is only possible in the perturbative limit, i.e., $\tau \ll 1$. The appropriate expression is[14]

$$\tau \cong \frac{\left(\lambda^2 - \frac{1}{\lambda}\right)\left\{\frac{\pi\rho\sigma^3}{\sqrt{3N}} - \frac{4}{N}\ln\left[1 + \frac{\pi\rho\sigma^3\sqrt{N}}{12\sqrt{3}}\right]\right\}}{120\left(1 - \frac{\pi\rho\sigma^3}{6\sqrt{3N}} - \frac{\pi^2\rho^2\sigma^6}{324}\right)} \quad (17)$$

Comparison of the perturbative result with full numerical calculations shows excellent agreement[14] up to $\tau \sim 0.2$. A close inspection of eq 17 reveals certain features of the order parameter. First, it is a supralinear function of segmental density, $\tau \sim (\rho\sigma^3)^x$, with an apparent exponent of $x \sim 1.3-1.4$. Second, to a good degree of approximation $\tau \sim N^{-1/2}$, which is a nonclassical power law that emerges due to finite size coupling of the correlation hole length scale ($\sim R_g \sim \sqrt{N}\sigma$) and the local segment scale in $g(r)$.[14] Comparison of our theoretical predictions with nuclear magnetic resonance (NMR) experiments and computer simulations on flexible polymer melts and concentrated solutions show good agreement.[14]

The stress exerted during uniaxial elongation is obtained by differentiating the total free energy with respect to strain, $\sigma_{total} = \lambda\partial F/\partial\lambda$. Often the parameter of interest in experiments is the reduced stress which quantifies the deviation from the classical strain dependence, $\lambda^2 - \lambda^{-1}$. PRISM theory yields for the reduced stress, in units of k_BT/σ^3

$$G \equiv \frac{\sigma_{total}}{\lambda^2 - \lambda^{-1}} = \frac{\rho\sigma^3}{N} + \frac{\rho\sigma^3 A}{24} - \left\{\rho\sigma^3 A^2\left\{\left(2\lambda^2 + \frac{1}{\lambda}\right)\left[2D + \frac{B}{12}\left(\lambda^2 + \frac{2}{\lambda} - 3\right) + \frac{A}{28}\left(\lambda^2 - \frac{1}{\lambda}\right)\right] - \frac{B}{12}\left(\lambda^2 - \frac{1}{\lambda}\right)^2\right\}\right\}\Big/\left\{3200\left[D + \frac{B}{24}\left(\lambda^2 + \frac{2}{\lambda} - 3\right) + \frac{A}{28}\left(\lambda^2 - \frac{1}{\lambda}\right)\right]^2\right\} \quad (18)$$

A λ dependence of the reduced stress is predicted in contrast to classical theories which ignore the strain-dependence of the excess (intermolecular) free energy. The linear elastic modulus is the reduced stress in the limit $\lambda \to 1$

$$E = \frac{3\rho\sigma^3}{N} + \frac{\rho\sigma^3\left\{\frac{\pi\rho\sigma^3}{\sqrt{3N}} - \frac{4}{N}\ln\left[1 + \frac{\pi\rho\sigma^3\sqrt{N}}{12\sqrt{3}}\right]\right\}}{8} - \frac{3\rho\sigma^3\left\{\frac{\pi\rho\sigma^3}{\sqrt{3N}} - \frac{4}{N}\ln\left[1 + \frac{\pi\rho\sigma^3\sqrt{N}}{12\sqrt{3}}\right]\right\}^2}{1600\left(1 - \frac{\pi\rho\sigma^3}{6\sqrt{3N}} - \frac{\pi^2\rho^2\sigma^6}{324}\right)}$$

$$\equiv E_{aff} + E_2 + E_3 \quad (19)$$

There are two nonclassical terms in eq 19. The first, E_2, is positive definite and is the entropic contribution of interchain repulsive (athermal) interactions to the elastic modulus in the absence of chain alignment. Deformation-induced alignment of the chains results in a decrease in free energy, and hence elastic modulus, and is quantified by the negative definite term, E_3. Note that these two nonclassical contributions to the modulus have different dependences on segmental density and N from their classical counterpart, E_{aff}. E_2 scales roughly quadratically with segmental density and inversely with $\sqrt{N}$, in contrast to the classical contribution which is linear in $\rho\sigma^3$ and inversely proportional to N. The dependence of E_3 on density is subtle due to the presence of $\rho\sigma^3$ in both the numerator and the denominator of eq 19. Well below the isotropic−nematic transition, $\rho\sigma^3 \ll (\rho\sigma^3)_{NI}$, E_3 is an approximately cubic function of segmental density, but because of the small numerical prefactor it is negligible compared to E_2. However as the liquid crystal transition density is approached, E_3 becomes dominant leading to significant reduction in the total elastic modulus, i.e., alignment-induced softening.

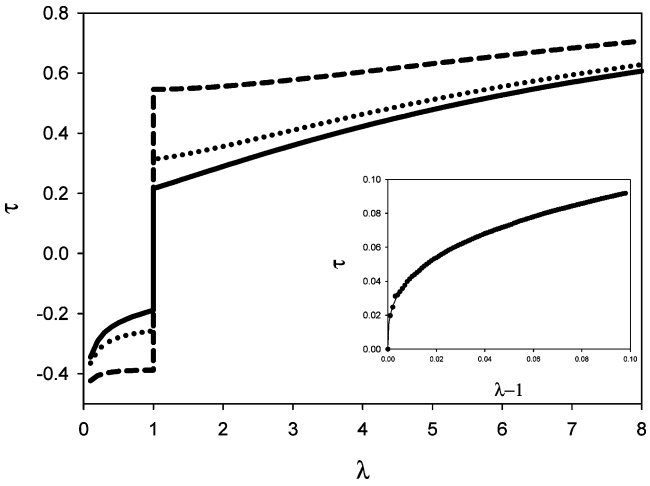

Figure 2. Variation of the induced orientational order parameter with strain at three segmental densites for $N = 100$: $\rho\sigma^3 = 5.6$ (solid), $\rho\sigma^3 = 6$ (dotted), and $\rho\sigma^3 = 8$ (dashed). The critical isotropic−nematic transition segmental density is 5.25. The inset shows the variation of the orientational parameter with extension at the strain free isotropic−nematic transition density. The line is a power law fit with an exponent ≈ 0.334.

III. Orientational Order and Density Fluctuations in Liquid Crystalline Elastomers

At high segmental densities, the perturbative calculation of the previous section breaks down; for example, inspection of eq 17 shows that τ diverges at the isotropic−nematic transition. The equilibrium segmental order at high density must then be determined by numerical minimization of the free energy. Figure 2 shows variation of the induced nematic order with uniaxial strain at three segmental densities above the (strain-free) LCP isotropic−nematic transition for $N = 100$ (unless stated otherwise, the degree of polymerization is taken to be 100 in all calculations). The strain free nematic order parameters at $\rho\sigma^3 = 5.6$, 6, and 8 are $\tau = 0.216$, 0.313, and 0.546, respectively, and $\tau = -0.188$, -0.257, and -0.388 in the discotic. We have restricted λ within the region of validity of the theory defined in eqs 10 and 11. The discontinuity at $\lambda = 1$ is due to the degeneracy of the nematic and discotic phases in the absence of strain. Introduction of strain leads to broken nematic−discotic symmetry, with extension favoring the nematic phase and compression the discotic. The λ-dependence of the induced segmental order decreases with segmental density because the chains are already significantly aligned in the absence of strain in both phases. The inset of Figure 2 shows the small strain behavior of the orientational order parameter at the critical (strain free) isotropic−nematic transition. The power law exponent is $^1/_3$, as expected given the mean field nature of our treatment of critical fluctuations (see Appendix A).

Figure 3 shows the continuous variation of the orientational order parameter with segmental density at three strains: $\lambda = 1.01$, 1.5, and 5. The segmental density for the emergence of significant values of τ decreases with strain. Of course, an

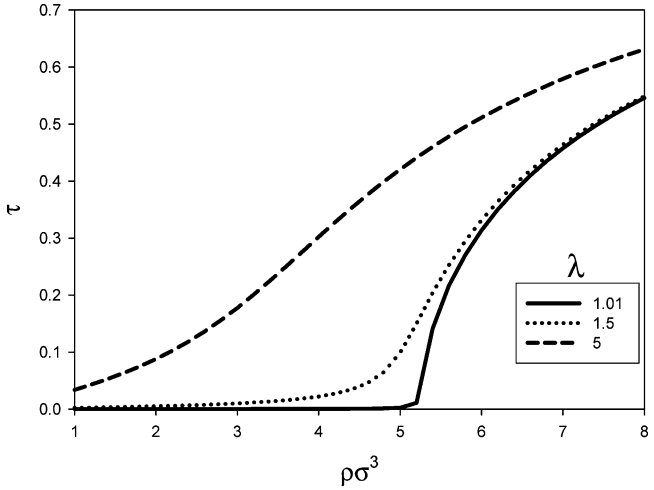

Figure 3. Orientational order parameter (for $N = 100$) as a function of segmental density at three strains.

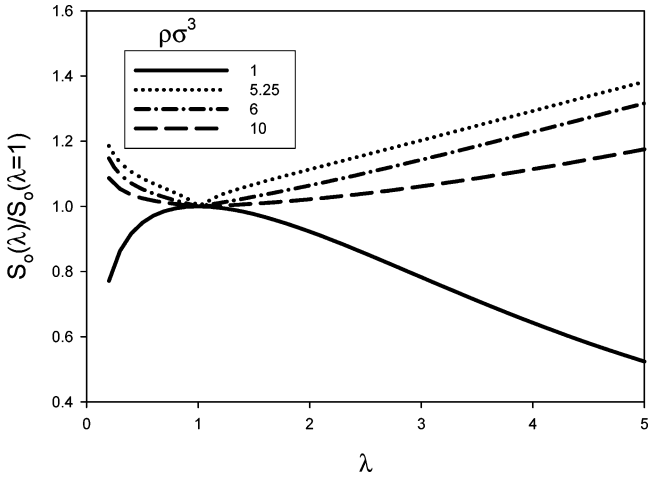

Figure 4. Dimensionless compressibility as a function of strain, $S_0(\lambda)$, normalized by its undeformed isotropic value, $S_0(\lambda = 1)$, at four segmental densities for a network strand size of $N = 100$. Here, $S_0(\lambda = 1) = 6.18$ at $\rho\sigma^3 = 1$, and $S_0(\lambda = 1) \approx 0.35$ at $\rho\sigma^3 = 5.25$, 6, and 10.

infinitesimal amount of strain will lead to nonzero values of τ at any density, i.e., a strained polymer network is "paranematic". For example, a network formed from an amorphous polymer like poly(dimethylsiloxane) ($\rho\sigma^3 = 1.0$) has a segmental order parameter of $\tau \sim 0.03$ at $\lambda = 5$. A "crossover density" can be defined as the point of maximum steepness, i.e., $\partial\tau/\partial\rho|_{\rho_c} =$ maximum. This density (not plotted) decreases with strain above a threshold value of λ, which is a function of N. For example $\rho_c\sigma^3$ decreases from approximately 5.1 (5.5) to 3.3 (5.0) as λ increases from 1 to 5 for $N = 50$ (500).

The dimensionless compressibility (or inverse bulk modulus) quantifies the amplitude of density fluctuations, $S_0 \equiv \rho k_B T \kappa_T \propto \langle(\delta\rho)^2\rangle/\rho^2$. In undeformed liquid crystalline polymers, alignment leads to a reduction in intermolecular contacts (interactions) and the excess free energy, and hence S_0 increases (more compressible). However in a deformed elastomer, a network strand not only aligns due to strain, its radius of gyration also increases resulting in a lower internal coil density. Hence, in contrast to alignment, chain deformation result in more repulsive intermolecular contacts. It is the complex interplay between these two effects that determines the change in the compressibility as an elastomer is strained. Figure 4 shows S_0 as a function of strain at four segmental densities $\rho\sigma^3 = 1$, 5.25, 6, and 10. At the lowest segmental density (paranematic), the degree of alignment

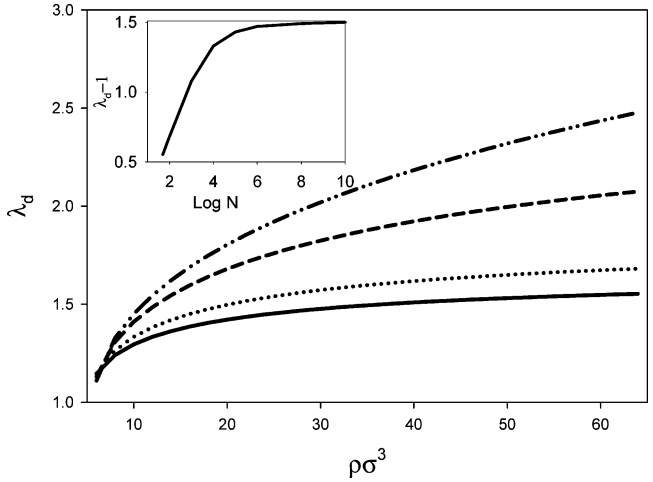

Figure 5. Spontaneous distortion as a function of the dimensionless segmental density at four network strand sizes: 50 (solid), 100 (dotted), 1000 (dashed), and $N \rightarrow \infty$ limit (dashed, double dotted). Inset shows the variation of the spontaneous distortion at maximum alignment with strand degree of polymerization.

is very small (see Figure 3), and hence, the net effect of strain is the suppression of density fluctuations; i.e., the elastomer hardens. A reverse trend is observed at higher densities (above the strain-free liquid crystal critical density) where the chain overlap caused by stretching is reduced by alignment, resulting in an enhancement of the compressibility. Note the cusp at the zero strain isotropic−nematic transition, $\rho\sigma^3 = 5.25$, marking the change in trends. At very high segmental densities (strong alignment), the strain induced softening effect necessarily diminishes.

IV. Mechanical Properties

As mentioned in the Introduction, liquid crystalline elastomers undergo a spontaneous increase in sample length along the director when they are cooled below their isotropic−nematic transition temperature. The magnitude of the spontaneous distortion is determined in our theory as the value of λ that minimizes the free energy, i.e., the value of $\lambda \equiv \lambda_d$ that corresponds to zero extension force. The variation of the spontaneous distortion with dimensionless segmental density at four strand degrees of polymerization is plotted in Figure 5. The distortion increases monotonically with density or degree of alignment. This trend is in agreement with experiments done on thermotropic liquid crystalline elastomers where a monotonic increase in spontaneous distortion is observed with enhanced orientation induced by a decrease in temperature. The maximum segmental alignment $\tau \rightarrow 1$ occurs at approximately $\rho\sigma^3 \approx 65$. The magnitude of the distortion increases with the polymer strand size. The inset of Figure 5 shows the variation with N of the spontaneous distortion at full alignment. This is a finite size effect with the asymptotic limit of $\lambda_d \rightarrow 2.5$ as $N \rightarrow \infty$. Subtle curve crossing occurs at the lowest densities due to the weak dependence of the isotropic−nematic transition density on the degree of polymerization (eq 15). Figure 6 shows that a mean field critical power law relation (with exponent $^1/_2$) between the spontaneous distortion and segmental density holds near the strain-free phase transition density (see Appendix A).

Because of the dearth of experimental data on lyotropic LCE, it is difficult to directly test our theoretical predictions for the spontaneous distortion. However, in experiments done on thermotropic LCE, a direct correlation between the spontaneous

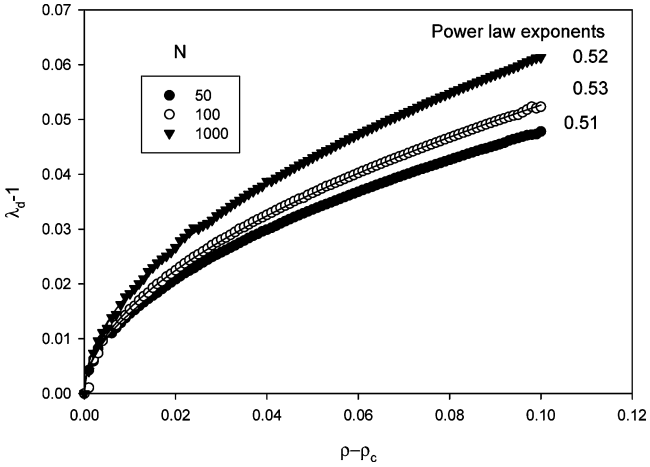

Figure 6. Scaling of the spontaneous distortion with segmental density deviation from its strain free critical value near threshold.

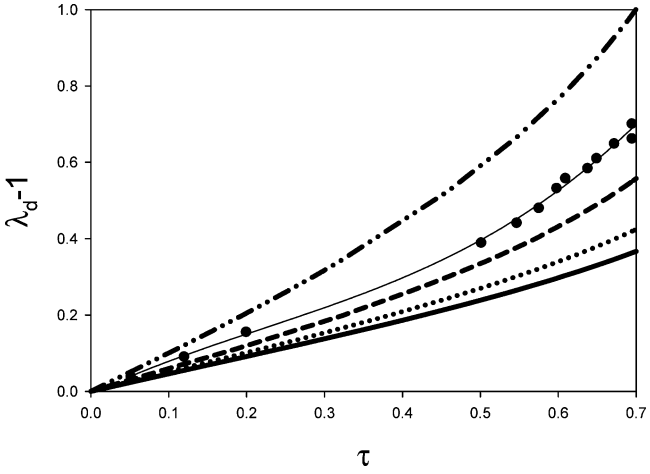

Figure 7. Comparison of the theoretical predictions of the spontaneous distortion as a function of segmental orientational order parameter with experiments on a thermotropic liquid crystalline elastomer (see text). Calculations are shown for $N = 100$ (solid), 250 (dotted), and $N \rightarrow \infty$ (dashed). The line through the experimental data (circle) is a cubic fit. The dashed double dotted line is the prediction of the neoclassical theory.[3]

distortion and the orientational order parameter has been established. We consider the experiments of Wermter and Finkelmann[5] on networks composed of polymethylhydrogensiloxane (PMHS) with side chain mesogen 4-but-3-enyloxybenzoic acid 4-methoxyphenyl ester. The crosslinking was done with a nematic polyester based on 1-(4-hydroxy-4′-biphenyl)-2-[4-(10-undecenyloxy)phenyl]butane which was end functionalized by vinyl groups. Because of its rigidity and length, the nematic crosslinker can be viewed as a main chain LC group whose nematogen also contributed to overall chain alignment. It was found that the resulting distortion depends strongly on the length and concentration of the crosslinking group, with a spontaneous distortion of up to a factor of 4 measured for 56 mol % of mesogenic main chain monomer units.

Figure 7 compares the theoretical spontaneous distortion as a function of the orientational order parameter for three LCE strand sizes against experiment. The order parameter variation in the theory is achieved by changing the segmental density. The concentration of the mesogen monomer unit in the experimental data shown is 20%; the strand length was not reported. This particular data set was chosen because it is the least rigid structure studied experimentally, and therefore

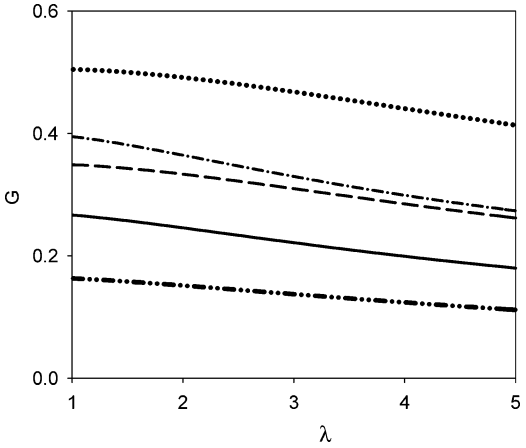

Figure 8. Reduced stress (units of $k_BT\sigma^{-3}$) as a function of strain at different segmental densities and strand lengths: $\rho\sigma^3 = 6$, $N = 100$ (solid); $\rho\sigma^3 = 8$, $N = 100$ (dashed); $\rho\sigma^3 = 12$, $N = 100$ (dotted); $\rho\sigma^3 = 6$, $N = 50$ (dashed and dotted); and $\rho\sigma^3 = 6$, $N = 250$ (dashed and double dotted). The corresponding values of the orientational order parameter as $\lambda \rightarrow 1^+$ are $\tau = 0.31$, 0.55, 0.72, 0.35, and 0.27, respectively.

represents the most appropriate for comparison with a thread chain model. The magnitude of the spontaneous distortion increases with the nematic order, and the theory captures the linear relationship at low τ. Deviation from linearity occurs at $\tau \approx 0.5$. Interestingly, both the theoretical predictions and the experimental data are well fitted by a cubic function over the entire τ range studied. The theoretical slopes at low τ range from 0.4 to 0.64, within a factor of 2 of the experimental value of 0.8. Clarke and co-workers[4] have also studied the effect of crosslinking on spontaneous distortion in siloxane based side chain nematic elastomers. They found that the slope of the linear regime varied from approximately 0.1 to 2.8, depending on the flexibility of the crosslinker. The conclusion reached in all these experiments is that the precise magnitude of the spontaneous distortion is strongly dependent on the molecular architecture, particularly the coupling of the nematic order of the main chain and side chain mesogens on the polymer backbone order, a nonuniversal chemical level feature not contained in our thread chain model. However, it is encouraging that the athermal thread based theory properly captures the trends observed in thermotropic liquid crystalline elastomers. The neoclassical theory[1,3] of nematic elastomers have also been successfully applied to understand spontaneous distortion (see Appendix B).

Figure 8 shows the reduced stress, G, defined in eq 18, as function of strain at different segmental densities and N under uniaxial extension. G decreases with λ, indicating strained induced softening opposite to the behavior of flexible polymer networks.[15] The magnitude of the softening is sensitive to the segmental density and strand length: the higher the density or N, the less pronounced the reduction in the reduced stress. A physical explanation is that strain induced orientation reduces the free energy cost of deformation. The effect is more pronounced for shorter chains and at densities closer to the zero strain isotropic−nematic transition (eq 14), because the *change* in the induced nematic order due to the applied strain is greater. Similar trends are seen under compression (not shown), but the magnitude of the decreases of G are far less, typically $\leq 10\%$ for λ as small as 0.2.

A plot of the reduced stress for $N = 100$ as a function of segmental density at three strain values is shown in Figure 9. The dips in the curves occur at the zero strain isotropic−nematic

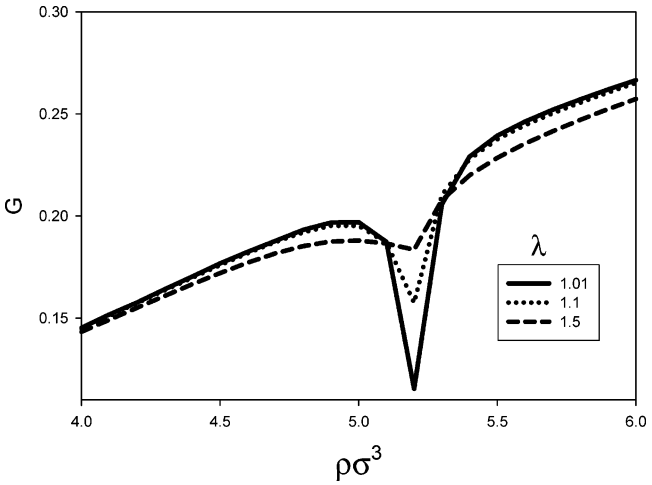

Figure 9. Variation of the reduced stress (units of $k_BT\sigma^{-3}$) with segmental density at three strain values and $N = 100$.

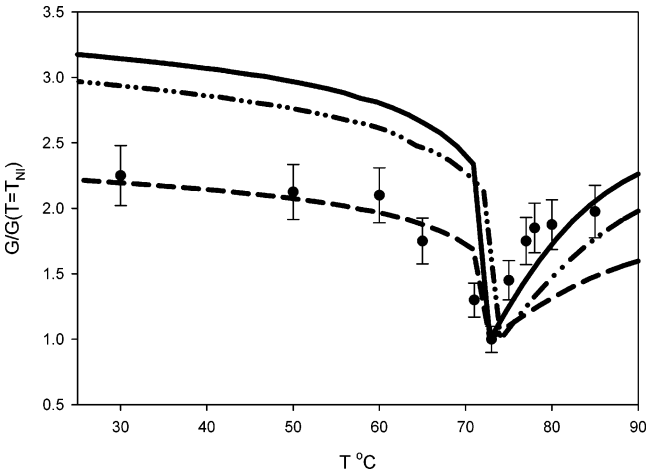

Figure 10. Comparison of the theoretical reduced stress as a function of temperature with experiments on a thermotropic LCE (see text): $\lambda = 1.04$, $N = 100$ (solid); $\lambda = 1.04$, $N = 50$ (dash double dot); and $\lambda = 1.06$, $N = 100$ (dash). The stress is normalized by its value at the strain free nematic phase transition temperature: 73 ($N = 100$) and 74 °C ($N = 50$).

transition density. It is much more pronounced at very small strain (linear modulus), where theoretically it diverges in the $\lambda \rightarrow 1$ limit (see Appendix A). In the numerical calculation, the dip becomes shallower as the imposed strain is increased, but the cusp does not vanish, even at very high λ or N. Only the location of the dip, in accordance with eq 15, and the magnitude of the modulus are affected by changes in the strand degree of polymerization. The monotonic growth of G with segmental density is recovered beyond the transition point, i.e., deep in the liquid crystalline state. The physical origin of the dip is the significant chain alignment, which drastically reduces the free energy cost of deformation. Recall that in section II the softening term (E_3) in the elastic modulus grows as a cubic function of density and becomes dominant around the liquid crystal transition. It formally diverges at the zero strain isotropic−nematic transition, an effect that would be "cut off" in a theory where the phase transition is first order.

The occurrence of a dip in the reduced stress around the zero strain isotropic−nematic transition has been observed in experiments on side chain thermotropic LCE.[16] To compare our theory with thermotropic LCEs, the segmental density is mapped to temperature space utilizing the following equation:

$$\rho - \rho_{NI} = \frac{\partial \rho}{\partial T}|T_{NI}(T - T_{NI}) \tag{20}$$

This implies the simple relation

$$\frac{T}{T_{NI}} = 1 + \frac{1}{\alpha_L T_{NI}}\left(1 - \frac{\rho}{\rho_{NI}}\right) \tag{21}$$

where α_L is the thermal expansion coefficient. In the experiments, the elastomer is composed of a side chain mesogen (M40CH3) connected to a PHMS backbone. The degree of polymerization of PHMS prior to cross-linking is 100. The isotropic−nematic temperature for the elastomer is 344 K, while the volume expansivity for a methylsiloxane based polymer is $\alpha_L \approx -10^{-3}\,K^{-1}$. Using these parameters our theoretical reduced stresses at $\lambda = 1.04$ and 1.06 at two strand lengths (50 and 100) are shown in Figure 10 along with the experimental results obtained at comparable λ values ($\lambda \approx 1.03 \pm 0.01$). The degree of polymerization has little effect on the prediction. The theory is in rather good agreement with the experiment. The contrasting predictions of the neoclassical theory[1,3] for the linear modulus are summarized in Appendix B.

V. Summary and Conclusion

We have developed a microscopic theory based on the Gaussian thread version of PRISM theory for the thermodynamics, structure and mechanical properties of liquid crystalline elastomers. The theory is "nonclassical" in the sense that it addresses the role of anisotropic interchain excluded volume interactions on the nematic order and mechanical response. Analytic expressions have been obtained for the free energy, orientational order, and elastic modulus. The theory also makes predictions for structure (interchain pair correlation functions) and compressibility. Deformation in the liquid crystalline state results in an increase of the dimensionless compressibility (strain softening) which is more pronounced as degree of polymerization and/or segmental density decrease.

The theory predicts a spontaneous distortion, λ_d, of the elastomer arising from the microscopic alignment of the chains due to anisotropic packing correlations. A direct correlation between it and the nematic order parameter emerges which is in good qualitative agreement with experiments on thermotropic liquid crystalline elastomers. The predicted dependence of λ_d on the chain degree of polymerization remains to be experimentally tested. The theory also predicts strain induced modulus softening due to the nonclassical (interchain) contribution to the free energy. This softening is particularly pronounced near the strain-free isotropic−nematic transition. Comparison of the theory with limited experiments on thermotropic elastomers shows rather good agreement.

There are several improvements that can be made to the current model and theory. One includes a more chemically realistic chain description. Since nematic elastomers are made up of rigid groups, incorporation of backbone stiffness and other local chemical aspects are likely needed for quantitative accuracy. Unfortunately, for anisotropic polymer liquids inclusion of chemically specific information beyond the thread model requires significantly more numerical effort. In contrast to the neoclassical theory, our approach as currently formulated is unable to address some important issues of LCE such as soft elasticity and a stripe instability arising from director rotation when strain is applied perpendicular to the nematic director.[1−3] This aspect could be addressed if any improvement to the single chain model (e.g. nonzero monomer diameter, chain stiffness)

which lifts the nematic−discotic degeneracy is made thereby resulting in a first-order phase transition.[22]

Acknowledgment. This paper is dedicated to Professor David Chandler: an outstanding teacher and mentor, and a pioneer in the area of statistical mechanics of liquids and soft matter. This work was supported by the U.S. Department of Energy, Division of Materials Sciences, under award number DEFG02-91ER45439, through the Frederick Seitz Materials Research Laboratory at the University of Illinois, Urbana−Champaign. We thank Professor Erik Luijten for discussions concerning Appendix A.

Appendix A: Analogy with Mean Field Theory

It was pointed out in section III that our theory predicts the orientational order at the isotropic−nematic transition density scales as $(\lambda - 1)^{1/3}$ for small strain. We showed also in section IV that the spontaneous distortion near threshold scales as the square root of the deviation of the segmental density from its strain free isotropic−nematic transition value. For a thermotropic LCE, the theory would give the same prediction for the scaling behavior of the spontaneous distortion with $(T - T_{NI})$. In the absence of strain, the orientational order near the phase transition scales with the segmental density[21] as $\tau \approx (1 - \rho_c/\rho)^{1/2}$. The critical exponents associated with these power laws are the classical mean field values[34] due to the deep analogy between a LCE and a magnet in an external magnetic field, H. For example, the temperature variation of the segmental order parameter at different strains has identical qualitative features as the spontaneous magnetization. Here, the external magnetic field plays the same role as the mechanical field in changing the curvature of the order parameter with temperature. Recall that in the absence of H, the spin system is also degenerate.

The reduced stress or modulus, a measure of the system response to external mechanical field, scales inversely as $(\rho\sigma^3 - \rho\sigma_{IN}^3)$ in neighborhood of the dip, $G \sim (\rho\sigma^3 - \rho\sigma_{NI}^3)^{-1}$. This is the expected mean field result which for a magnet corresponds to the variation of susceptibility with temperature as $\chi \sim (T - T_c)^{-1}$.

Appendix B: Neoclassical Theory of Nematic Elastomers

Warner and co-workers[3] have developed a theory of nematic elastomers which combines elements of the Landau−de Gennes theory of liquid crystals with classical rubber elasticity. In their theory, the network strand end-to-end distance is assumed to obey an anisotropic Gaussian distribution, with different effective step lengths in directions parallel and perpendicular to the director or strain axis, $\sigma_\parallel \neq \sigma_\perp$. The theory predicts for the spontaneous distortion below the isotropic−nematic transition temperature

$$\lambda_d = \left(\frac{\sigma_\parallel}{\sigma_\perp}\right)^{1/3} \tag{B1}$$

To make contact with the nematic order parameter, a specific polymer chain model is required. For a freely jointed chain, $\sigma_\parallel = (1 + 2\tau)\sigma_o$ and $\sigma_\perp = (1 - \tau)\sigma_o$, where σ_o is the isotropic step length, thereby yielding[16]

$$\lambda_d = \left(\frac{1 + 2\tau}{1 - \tau}\right)^{1/3} \tag{B2}$$

Hence, in contrast to our theory, the neoclassical model predicts a spontaneous distortion that is independent of the strand length. Figure 7 compares the prediction of this model with experimental data and our theory. The neoclassical theory predicts linear behavior at small τ, with a slope of unity, which is larger by a factor of ~ 2 than our results at $N = 100$. The simple theory is in rather surprisingly good agreement with experiment. Its predicted λ_d is also roughly cubic up to $\tau \sim 0.75$, but formally diverges as $\tau \to 1$.

The neoclassical theory predicts for the linear elastic modulus[16]

$$E_{nc} = \mu\left[1 - \frac{3\mu}{(1 + \tau - 2\tau^2)^2}\left(\frac{\partial^2 F_{LD}}{\partial \tau^2}\right)^{-1}\right] \tag{B3}$$

where μ is the shear modulus and F_{LD} is the modified phenomenological Landau−de Gennes free energy. For the phantom chain model, the shear modulus is given by

$$\mu = \frac{\rho k_B T}{N} = \frac{\rho\sigma^3}{N}\left(\frac{k_B T}{\sigma_o^3}\right) \tag{B4}$$

The neoclassical theory assumes that the isotropic−nematic transition of the rubber network is first order and thereby calculates the coefficients of the Landau−de Gennes free energy by fitting experimental data, e.g. enthalpy of the phase transition. Within this formulation, the second derivative of the Landau−de Gennes free energy is[16]

$$\frac{\partial^2 F_{LD}}{\partial \tau^2} = \frac{4\Delta S}{\tau_{NI}}\left[T^* - T + \frac{3}{2}\frac{\tau(T)}{\tau_{NI}}(T_{NI} - T^*)\right] \tag{B5}$$

Here ΔS and τ_{NI} are the change in entropy density and order parameter at the phase transition, respectively, and T^* is the temperature below which the isotropic state is unstable, i.e., the limit to supercooling. Typically,[1,16] $T_{NI} - T^* \sim 1K$. Inspection of eqs B3−B5 shows that the neoclassical theory also predicts a reduction in the modulus from its classical value around the phase transition arising from the mechanical-nematic coupling. However, the neoclassical theory fails in its prediction of the modulus at temperatures above the transition (i.e. in the paranematic phase) primarily because it assumes the transition is first order, in contradiction to experiments on nematic elastomers which show a continuous transition. Attempts to empirically reconcile these differences by incorporating experimental data for $\tau(T)$, or by computing the Landau free energy coefficients around a "critical" temperature defined as the maximum slope of $\tau(T)$, lead to results that are either quantitatively poor or have unphysical features.[35] Confrontation of the neoclassical theory with the modulus data in Figure 10 has not been done.

References and Notes

(1) Warner, M.; Terentjev, E. M. *Liquid Crystal Elastomers*; Oxford University Press: Oxford, England, 2003.
(2) Terentjev, E. M. *J. Phys. Condens. Matter* **1999**, *11*, R239.
(3) Warner, M.; Terentjev, E. M. *Prog. Polym. Sci.* **1996**, *21*, 853.
(4) Clarke, S. M.; Hotta, A.; Tajbakhsh, A. R.; Terentjev, E. M. *Phys. Rev. E* **2001**, *64*, 061702.
(5) Wermter, H.; Finkelmann, H. *e-Polymers* **2001**, *13*.
(6) Rubinstein, M.; Colby, R. H. *Polymer Physics*; Oxford University Press: Oxford, England, 2003.
(7) Mark, J. E.; Erman, B. *Rubberlike Elasticity: A Molecular Primer*; John Wiley & Sons: New York, 1988.
(8) Rubinstein, M.; Panyukov, S. *Macromolecules* **2002**, *35*, 6670.
(9) Edwards, S. F.; Vilgis, T. A. *Rep. Prog. Phys.* **1988**, *51*, 243.
(10) Ronca, G.; Allegra, G. *J. Chem. Phys.* **1975**, *63*, 4990.
(11) Ball, R. C.; Doi, M.; Edwards, S. F.; Warner, M. *Polymer* **1981**, *22*, 1010.
(12) Graessley, W. W. *Adv. Polym. Sci.* **1974**, *16*, 1.
(13) Kutter, S.; Terentjev, E. M. *Eur. J. Phys. E* **2001**, *6*, 221.
(14) Oyerokun, F. T.; Schweizer, K. S. *J. Chem. Phys.* **2004**, *120*, 475.
(15) Oyerokun, F. T.; Schweizer, K. S. *J Chem. Phys.* **2004**, *120*, 9359.

(16) Finkelmann, H.; Greve, A.; Warner, M. *Eur. J. Phys. E* **2001**, *5*, 281.
(17) Chandler, D.; Andersen, H. C. *J. Chem. Phys.* **1972**, *57*, 1930.
(18) Chandler, D. In *Liquid State of Matter: Fluids, Simple and Complex*; Montroll, E. W., Lebowitz, J. L., Eds.; North-Holland Publishing Company: Amsterdam, 1982; p 275.
(19) Schweizer, K. S.; Curro, J. G. *Adv. Chem. Phys.* **1997**, *98*, 1.
(20) Schweizer, K. S.; Curro, J. G. *Adv. Polym. Sci.* **1994**, *116*, 319.
(21) Pickett, G. T.; Schweizer, K. S. *J. Chem. Phys.* **1999**, *110*, 6597.
(22) Pickett, G. T.; Schweizer, K. S. *J. Chem. Phys.* **2000**, *112*, 4869.
(23) Pickett, G. T.; Schweizer, K. S. *J. Chem. Phys.* **2000**, *112*, 4881.
(24) Fuchs, M.; Schweizer, K. S. *J. Phys. Cond. Matter* **2002**, *14*, R239.
(25) Hooper, J. B.; Schweizer, K. S.; Desai, T.; Koshy, R.; Keblinski, P. *J Chem. Phys.* **2004**, *121*, 6986.
(26) Schweizer, K. S.; Curro, J. G. *Macromolecules* **1988**, *21*, 3070.
(27) Schweizer, K. S.; Curro, J. G. *Macromolecules* **1988**, *21*, 3082.
(28) Doi, M.; Edwards, S. F. *The Theory of Polymer Dynamics*; Clarendon Press: Oxford, England, 1986.
(29) Fetters, L. J.; Lohse, D. J.; Richter, D.; Witten, T. A.; Zirkel, A. *Macromolecules* **1994**, *27*, 4639.
(30) Hansen, J.-P.; McDonald, I. R. *Theory of Simple Liquids*, 2nd ed.; Academic Press: San Diego, CA, 1986.
(31) Chandler, D. *Phys. Rev. E* **1993**, *48*, 2898.
(32) Fuchs, M. *Z. Phys. B* **1997**, *103*, 521.
(33) Wall, F. T.; Flory, P. J. *J. Chem. Phys.* **1951**, *19*, 1435.
(34) Goldenfeld, N. *Lectures on Phase Transitions and the Renormalization Group*; Addison-Wesley Publishing Co.: Reading, MA, 1992.
(35) Pereira, G. G.; Warner, M. *Eur. J. Phys. E* **2001**, *5*, 295.